Polymer 51 (2010) 5680–5687

Contents lists available at ScienceDirect

Polymer

journal homepage: www.elsevier.com/locate/polymer

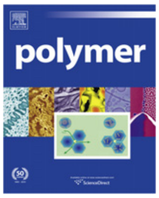

Synthesis by self-condensing AGET ATRP and solution properties of *arborescent* poly(sodium 2-acrylamido-2-methyl-*N*-propane sulfonate)

Daniel Gromadzki [a,b,*], Alexey Tereshchenko [a], Ričardas Makuška [a]

[a] *Department of Polymer Chemistry, Vilnius University, Naugarduko 24, LT-03225 Vilnius, Lithuania*
[b] *Department of Supramolecular Polymer Systems, Institute of Macromolecular Chemistry, Academy of Sciences of The Czech Republic, Heyrovsky Sq. 2, 162 06 Prague 6, Czech Republic*

ARTICLE INFO

Article history:
Received 19 June 2010
Received in revised form
4 September 2010
Accepted 20 September 2010
Available online 29 September 2010

Keywords:
Arborescent polyelectrolytes
Self-condensing AGET ATRP
Conformation

ABSTRACT

Randomly branched (*arborescent*) poly(sodium 2-acrylamido-2-methyl-*N*-propanesulfonates) (NaPAMPS) were synthesized via self-condensing vinyl polymerization using activators generated by electron transfer atom transfer radical polymerization (AGET ATRP). The controlled self-condensing AGET ATRP of NaAMPS was realized in the presence of 2-(2-bromopropionyloxy)ethyl acrylate (BPEA) as a branching monomer (*inimer*) in water/pyridine (35–50% of Py) mixed solvents. The content of BPEA in the reaction feed was varied from 10 to 30 wt% allowing the synthesis of NaPAMPS with different degree of branching. SEC determined molecular weight of the prepared NaPAMPS was $M_w = 94\ 000–120\ 000$ g/mol, and the accompanying polydispersity index PDI ranged from 1.84 to 2.47. The definite evidence of highly branched structure of NaPAMPS was provided by the dependence of radius of gyration R_g on weight-average molecular weight M_w with characteristic slope $a = 0.38–0.42$, and by small-angle X-ray scattering (SAXS) analysis. Molecular parameters, conformation and dynamics of the branched NaPAMPS in dilute salt-free solutions and in the presence of a salt were elucidated by static and dynamic light scattering and SAXS.

1. Introduction

Polyelectrolytes are very important polymeric derivatives because of their wide range of applications in colloid chemistry, biological and technological processes [1]. Since more than a decade from its discovery, controlled/living radical polymerization (CLRP) [2] encompassing nitroxide-mediated radical polymerization (NMP) [3], atom transfer radical polymerization (ATRP) [4] and reversible addition-fragmentation chain transfer polymerization (RAFT) [5] continue to demonstrate its tremendous potential in the preparation of polymers with complex architectures, controlled molecular weights and low polydispersities [6–8]. Fréchet *et al.*[9] in 1995 introduced the concept of self-condensing vinyl polymerization (SCVP) allowing facile synthesis of highly branched and hyperbranched macromolecules in a one–pot reaction. Following this seminal report, SCVP concept has been applied to various polymerization mechanisms including living cationic [10], anionic [11], group-transfer [12], NMP [13], ATRP [14–17], RAFT [18], thiol-yne chemistry [19] and others. The present article reports for the first time the synthesis of strong branched polyelectrolytes utilizing self-condensing AGET ATRP mechanism [20]. The interest in branched polymers arises from the fact that their bulk and solution properties are very different from those of linear analogues of the same molecular weight [21]. In the case of polyelectrolytes, solution behavior becomes more complex due to repulsive electrostatic interactions of adjacent charged monomeric units on the polymeric backbone which tends to adopt more extended, rigid-rod-like conformation [22].

The direct synthesis of well-defined polyelectrolytes or block copolymers containing acidic segments is very difficult since most living polymerization mediating agents are sensitive to acidic conditions. This obstacle can be circumvented by selective post-functionalization of one block of a copolymer prepared by living polymerization, for example, sulfonation of polystyrene [23], tetrazolation (azide-nitrile click chemistry) of acrylonitrile units [24] or a deprotection of corresponding ester [25]. Indeed, reports on the synthesis of poly(2-acrylamido-2-methyl-*N*-propane sulfonate) (PAMPS) of controlled architecture are scarce. Recently, successful CLRP of 2-acrylamido-2-methyl-*N*-propane sulfonate (AMPS) has been demonstrated by ATRP and RAFT methods. Crescenzi et al.[26] described ATRP of sodium salt of AMPS (NaAMPS) using tris

---

[*] Corresponding author. Current address: Fundamentals of Advanced Materials Group, Faculty of Aerospace Engineering, Delft University of Technology, Kluyverweg-1, 2629 HS Delft, The Netherlands. Tel.: +31 15 2784559; fax: +31 15 2784472.
E-mail address: D.Gromadzki@tudelft.nl (D. Gromadzki).

0032-3861/$ – see front matter © 2010 Elsevier Ltd. All rights reserved.
doi:10.1016/j.polymer.2010.09.058

[2-(dimethylamino)ethyl]-amine (Me$_6$TREN) and copper (I) chloride (CuCl) catalytic system in 50:50 solvent mixture of DMF and water. Dubois et al.[27] conducted aqueous ATRP of NaAMPS to prepare well-defined poly(ethylene oxide)-*block*-(sodium 2-acryl amido-2-methyl-N-propane sulfonate) starting from poly(ethylene oxide) macroinitiator. Matyjaszewski and coworkers reported polymerization of 2-acrylamido-2-*N*-propanesulfonic acid (AMPSA) via ATRP using CuCl/2,2′-bipyridine (bpy) catalyst complex followed by *in situ* neutralization of the acidic proton in AMPSA with tri(*n*-butyl)amine (TBA) and incorporation of AMPSA segment into block and molecular brush architecture [28]. RAFT was employed for controlled homopolymerization of AMPS in water using [4,4′-azo bis(4-cyanopentanoic acid) as initiator and 4-cyanopentanoic acid dithiobenzoate as the RAFT chain transfer agent by McCormick et al.[29].

PAMPS belongs to a class of strong polyelectrolytes which upon dissolution in water exhibits high degrees of ionization and extensive coil expansion. Upon addition of salt the electrostatic interactions among monomeric units become screened, and the polyelectrolyte eventually behaves like neutral polymer [30]. The chain characteristics in dilute solutions including static and dynamic parameters of linear PAMPS prepared by conventional radical polymerization were elucidated by light scattering and viscometry [31,32]. As far as the branched polyelectrolyte architecture is concerned, we are not aware of any published work on NaPAMPS. This prompted us to report molecular parameters and solution properties of the branched NaPAMPS synthesized by AGET ATRP of NaAMPS in the presence of 2-(2-bromopropionyloxy)ethyl acrylate (BPEA) which served as a branching monomer (*inimer*).

2. Experimental

2.1. Materials

Benzene was refluxed over CaH$_2$ followed by distillation in N$_2$ atmosphere. Pyridine and triethylamine were stored over NaOH prior to use. 2-Acrylamido-2-methylpropanesulfonic acid (AMPS), ethyl 2-bromoisobutyrate (EBiB), 2-hydroxyethyl acrylate (HEMA), 2-bromopropionyl bromide, 1,1,4,7,10,10-hexamethyltriethylenetetramine (HMTETA), CuBr$_2$, hydroquinone, ascorbic acid (AscA) and NaOH were purchased from Aldrich and used as received.

2.2. Synthesis

2.2.1. Synthesis of 2-(2-bromopropionyloxy)ethyl acrylate (BPEA)

Synthesis of BPEA *inimer* was accomplished according to previously published procedure [33]. Caution: precursors and product are light sensitive. A 1L 4-neck round-bottomed flask, equipped with mechanical stirrer, condenser and drop funnel, was purged with nitrogen and placed into an ice/water bath. 2-Hydroxyethyl acrylate (42 ml, 0.4 mol), triethylamine (63 ml, 0.44 mol) and dry benzene (250 ml) were placed into the flask. A mixture of 2-bromopropionyl bromide (44 ml, 0.41 mol) and dry benzene (100 ml) was added dropwise. Then the cooling bath was removed and the reaction mixture was stirred at room temperature for 3 h. Subsequently, the solution was filtered, washed with water and Na$_2$SO$_4$ (aq). Organic layer was separated and stored over anhydrous Na$_2$SO$_4$ over night. Then product was stabilized with hydroquinone (50 mg) and benzene was evaporated. The brown liquid residue was distilled under vacuum (140–146 °C/15 mm) to obtain a yellowish product which was passed through alumina column (eluent CH$_2$Cl$_2$). After removal of the solvent, a colourless liquid has been obtained. Yield 59 g (59%). ^{1}H NMR (*δ*, ppm, *d*-chloroform): 1.85 (d, 3H, CH$_3$,), 4.43 (m, 5H, CH$_2$O and CHBr), 5.89 and 6.46 (d, 2H, CH$_2$=), 6.16 (m, 1H, CH).

2.2.2. Synthesis of branched copolymers of AMPS and BPEA

Sample NaPAMPS-6 (Table 1). NaOH (0.35 g, 8.75 mmol) was dissolved in distilled water (4 ml) in a 25 ml round-bottomed flask. AMPS (1.8 g, 8.69 mmol) was added to the solution upon stirring and cooling in water bath. The solution's pH was adjusted to 7.5 by addition of solid NaOH. Then BPEA (0.2423 g, 0.965 mmol), pyridine (4 ml), HMTETA (26.2 μl, 96.4 μmol) and CuBr$_2$ (0.0216 g, 96.7 μmol) were added into the flask. The solution was purged with nitrogen for 40 min. The initiator EBiB (7.2 μl, 48 μmol) was introduced and the mixture was purged again for 10 min. Subsequently, ascorbic acid (0.0085 g, 48.3 μmol) was added and dissolved upon intensive stirring. The reaction was performed at room temperature in tightly closed flask. The reaction was quenched after 40 min by passing air through the solution. The polymer was purified by dialysis against distilled water (2 days), concentrated, dissolved in methanol and passed through silicagel column. After that, polymer was dialyzed against water for 2 days. A solid product was obtained after concentration followed by drying under vacuum.

Sample NaPAMPS-9 (Table 1). Similar as for the sample NaPAMPS-6 but the solvents ratio was changed (water 5 ml and pyridine 3 ml).

Sample NaPAMPS-17 (Table 1). Similar as for the sample NaPAMPS-6 but the monomers ratio was changed (AMPS 1.6 g, 7.72 mmol and BPEA 0.4846 g, 1.93 mmol).

Sample NaPAMPS-24 (Table 1). Similar as for the sample NaPAMPS-6 but the monomers ratio was changed (AMPS 1.47g, 7.09 mmol and BPEA 0.7632g, 3.04 mmol).

2.3. Characterization

2.3.1. ^{1}H NMR spectroscopy

The ^{1}H NMR spectra of NaPAMPS in D$_2$O were recorded on a UNITY INOVA VARIAN spectrometer (300 MHz). The content of BPEA units (mol.%) in branched NaPAMPS was calculated by two independent methods: 1) according to the intensity (integral) of the signals at 4.15 ppm (I$_{4.15}$) and 3.7 ppm (I$_{3.7}$) corresponding to protons in oxymethylene groups of BPEA and sulfonmethylene groups of NaAMPS, respectively; 2) by comparing the peak integration of the signals at 4.15 ppm and 1.98 ppm (I$_{1.98}$) where the

Table 1

Synthesis of randomly branched NaPAMPS under AGET ATRP conditions. Total concentration of the monomers $\Sigma[M] = 1.2$ mol/l, [EBIB] = 0.006 mol/l, $\Sigma[M]:[CuBr_2]:[HMTETA]:[ASCA] = 200:2:2:1$, room temperature, the reaction time 40 min.

Sample	AMPS: BPEA, mol%	Water: Pyridine	Conv., %	Elemental analysis		BPEA units, mol%	
				N	S	N, S	NMR
NaPAMPS-6	90:10	1:1	64	4.95	10.32	28	6
NaPAMPS-9	90:10	5:3	65	5.01	9.99	28	9
NaPAMPS-17	80:20	1:1	59	4.63	9.35	35	17
NaPAMPS-24	70:30	1:1	57	4.48	9.23	37	24

latter corresponds to the protons in methyne groups of the main-chain present in both NaAMPS and BPEA:

$$m_{BPEA} = \frac{I_{4.15}}{I_{4.15} + I_{3.7}} \cdot 100\% \qquad (1)$$

$$m_{BPEA} = \frac{I_{4.15}}{2 \cdot I_{1.98}} \cdot 100\% \qquad (2)$$

2.3.2. *Size exclusion chromatography (SEC)*[34]

The modular chromatograph consisted of a Degasser X-act (Your Research, Onsala, Sweden), a Constametric® 3200 MS pump (Thermo Separation Products, Riviera Beach, FL), a V-451 PEEK six port injection valve with 100 µl loop (Upchurch Scientific, Oak Harbor, WA, USA), a DAWN-DSP multi-angle light scattering photometer (Wyatt Technology, Santa Barbara, CA, USA). Simultaneous concentration detection was performed using an R-401 differential refractometer (Waters Assoc., Milford, MA, USA). Filtered toluene (Merck, Darmstadt, Germany) was employed for calibration of the MALS detector and sodium chloride for calibration of the refractive index detector. The detectors at different angles in the MALS instrument were normalized to the 90° detector using a narrow pullulan standard P-50 (Shodex standard P-82, Showa Denko, Tokyo, Japan). The signals from the two detectors were analyzed by ASTRA software (ASTRA for Windows 4.50) (Wyatt Technology, Santa Barbara, CA, USA). The angular dependence of the scattered light was extrapolated to zero angle using the linear Berry fit method to obtain molar mass and radius of gyration as a function of elution volume. The effect of the second virial coefficient may be neglected because of very low concentration of eluted species in a SEC experiment. The refractive index increment $dn/dc = 0.132$ ml/g was used in the calculations. The recovery was obtained from the ratio of the mass eluted from the column (determined by integration of the refractometer signal) to the mass injected. The mobile phase was always a 0.1 M sodium chloride solution which was 3 mM in sodium azide.

A set of three columns (8×250 mm) in series packed with hydrophilized GMB 200, 1000, 5000 + poly(glycidyl methacrylate) packings (Labio, Prague, Czech Republic), particle size 10 µm, having for poly (ethylene oxide) a linear calibration in terms of log *M* vs. elution volume from 2×10^4 extended above 5×10^6, was used for centrifuged as well as filtered samples. A TSK-GEL column GMPW 5000, 7.8×600 mm, particle size 17 µm, molar mass separation range 4000–1×10^6 for poly (ethylene oxide) was used for the analysis of filtered samples.

2.3.3. *Light-scattering measurements*

Solutions of the branched polyelectrolytes were investigated by dynamic light scattering (DLS) using an ALV CGE photogoniometer equipped with a Uniphase 22 mW HeNe laser and an ALV6010 correlator. The measured intensity correlation curves $g^2(t)$ were converted into distributions $A(\tau)$ of relaxation times τ using the inverse Laplace transformation

$$g^2(t) = 1 + \beta\left[\int A(\tau)\exp(-t/\tau)d\tau\right]^2, \qquad (3)$$

where t is the delay time of the correlation function and β is an instrumental parameter. The programme REPES was used to perform the inverse Laplace transformation in Eq.(3). The relaxation time τ is related to the diffusion coefficient D by the relation $D = (\tau q^2)^{-1}$ where q is the scattering vector. The hydrodynamic radius R_h of the particles is calculated from the diffusion coefficient using the Stokes–Einstein equation

$$D = k_B T / 6\pi\eta R_h, \qquad (4)$$

where T is the absolute temperature, η is the viscosity of the solvent and k_B is the Boltzmann constant.

The weight-average molecular weight (M_w), the second virial coefficient (A_2) and the radius of gyration (R_g) of the hyperbranched polyelectrolyte were determined by static light scattering (SLS; He-Ne laser $\lambda_0 = 632.8$ nm) in 0.15 NaCl aqueous solution at 25 °C with the Zimm procedure. The refractive index increment (dn/dc) of polymer was 0.132 ml/g. The scattering angle was in the range 30–150°.

2.3.4. *Small-angle X-ray scattering (SAXS)*

SAXS experiments were performed using a pinhole camera (Molecular Metrology SAXS System) attached to a microfocused X-ray beam generator (Osmic MicroMax 002) operating at 45 kV and 0.66 mA (30 W). The camera was equipped with a multiwire, gas-filled area detector with an active area diameter of 20 cm (Gabriel design). Two experimental setups were used to cover the q range of 0.007–1.1 Å^{-1} ($q = (4\pi/\lambda)\sin(\theta/2)$, where λ is the wavelength and θ is the scattering angle). The scattering intensities were put on absolute scale using a glassy carbon standard. Prior to fitting analysis the solvent scattering had been subtracted.

3. Results and discussion

3.1. *Synthesis of arborescent poly(sodium 2-acrylamido-2-methyl-N-propane sulfonate)*

Recently, synthesis of linear AMPS homopolymers, and AMPS containing block [25] and brush copolymers by ATRP has been reported [24,26], however, the synthesis of highly branched (*arborescent*) polyelectolytes based on AMPS monomer was not yet described. Conventional ATRP cannot be performed in acidic solutions of AMPS because of interference of sulfonic acid groups with nitrogen of an ATRP ligand leading to decomposition of copper/ligand complex and complexation of acrylamide group with copper catalyst [24,25,27]; moreover, AMPS when not fully neutralized exhibits significant autoinitiation effect in water [35]. In order to eliminate the above undesirable effects, AMPS was converted to the sodium salt (NaAMPS). A co-monomer BPEA synthesized by the known method [26] acted as an *inimer* (*ini*tiator-mono*mer*) unit under ATRP conditions (Fig. 1). Several other parameters need to be considered while setting up aqueous copper-mediated ATRP synthesis of branched polyelectrolytes. For example, it was challenging to find an appropriate solvent to maintain the reaction mixture with rather high content of BPEA (up to 30%) homogeneous. The mixture of water and pyridine (1:1 to 2:1, wt.) yielded homogenous solutions and was suitable for the polymerization. Since Cu(I) complexes are less soluble in water than corresponding Cu(II) complexes and are subject to disproportionation, they were generated *in situ* by reduction of Cu(II) using ascorbic acid. AGET ATRP allows fast formation of catalytic complex from the soluble Cu (II) salt which is useful for polymerization in water. Activity of Cu(I) complex was secured by the ligand HMTETA. Choosing active initiator EBiB and active Cu(I) complex, we had an intention to reduce selectivity of the propagation reaction and thus minimize a difference in reactivity ratios of the monomers.

A series of branched copolymers based on NaAMPS has been synthesized under AGET ATRP conditions (Table 1). Because of different amount of BPEA in the reaction mixture, the copolymers were expected to be of different degree of branching.

Self-condensing AGET ATRP proceeded very fast – after 2 min from the start the reaction mixture containing 10% of BPEA became opalescent and after 5 min it became two-phase excluding swollen polymer as a precipitate. Although no visible changes were observed afterwards, the reaction was allowed to proceed for

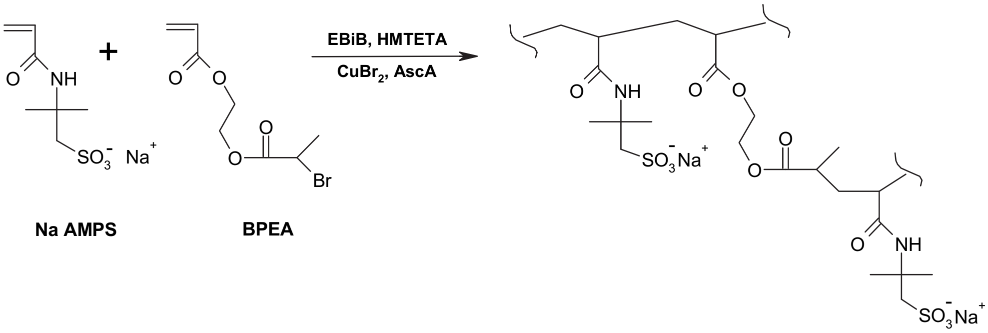

Fig. 1. Self-condensing AGET ATRP of NaAMPS using BPEA as an *inimer*.

40 min. In the case of the monomer mixture containing 30% of BPEA, the opalescence was observed after 25 min, but the solution became viscous after 5 min from the start. In order to avoid precipitation of the formed polymer, copolymerization of the monomer mixture AMPS:BPEA = 90:10 mol% was repeated using the solvent with lower content of pyridine (the sample NaPAMPS-9). The monomers were still soluble in the reaction mixture but the effect of the solvent on solubility of the resulting polymer was negligible, i.e. it precipitated but several minutes later.

The conversions of the monomers were moderate (57–65%, Table 1) which is related, probably, to heterogeneity of the system occurring during polymerization. On the other hand, moderate conversions are preferable attempting to avoid possible gellation of the reaction mixture and also full consumption of more reactive AMPS at high conversions.

The content of BPEA units in the branched NaPAMPS was calculated using ^{1}H NMR spectroscopy. Strong signal at 1.40 ppm attributed to the protons of two methyl groups in NaAMPS units prevails in the spectra (Fig. 2). This signal overlaps with the signal of methylene protons (1.5–1.6 ppm) of the mainchain. Fortunately, other signals are well resolved and can serve as analytical. The signal at 3.27 ppm belongs to the protons in $-CH_2$-SO_3 group of NaAMPS units while the signals at 3.73 ppm and 4.15 ppm are attributed to the protons present in two oxymethylene groups of BPEA units. The content of BPEA units (mol.%) was calculated from the ratio between the peak integration of the protons from oxymethylene groups of BPEA at 4.15 ppm and from sulfonmethylene groups of NaAMPS at 3.27 ppm, and was verified by comparing the peak integration of the signals at 4.15 ppm and 1.98 ppm. The signal at 1.98 ppm belongs to the protons in methynegroups of the mainchain present in both NaAMPS and BPEA, and its intensity does not depend on composition of the copolymer (branching). The content of BPEA units was lower compared to the content of BPEA in the monomer feed (Table 1). Nevertheless, changing ratio of the monomers in initial monomer feed, branched NaPAMS with the content of BPEA units from 6 to 24 mol% were synthesized.

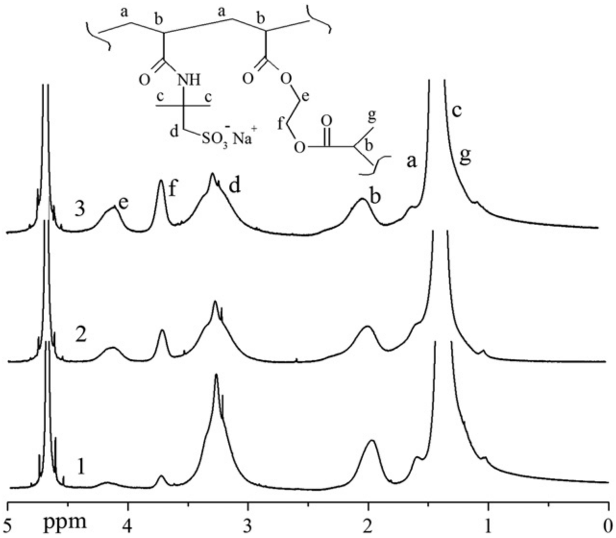

Fig. 2. ^{1}H NMR spectra of NaPAMPS-6 (1), NaPAMPS-17 (2) and NaPAMPS-24 (3) in D_2O.

The copolymer composition calculated from elemental analysis (average value from both N and S content, Table 1) was rather different from that calculated from ^{1}H NMR spectroscopy. Considerably lower content of AMPS units determined by elemental analysis is apparently related to high hygroscopicity of branched PAMPS polyelectrolytes. Branched PAMPS contained certain amount of water which distorted results of elemental analysis. Because of hygroscopicity of the polymers as well as small variation in the content of N and S, elemental analysis was found unsuitable for determination of BPEA units in branched PAMPS. In contrast, ^{1}H NMR spectroscopy gave reliable and reproducible results.

It is evident from the polymer compositions shown in Table 1 that AMPS has higher reactivity than BPEA. The difference between compositions of monomer feeds and corresponding copolymer compositions is not large, however, giving an idea that reactivity ratios of these co-monomers are not very different thus excluding formation of AMPS homopolymer. The copolymers apparently do not contain homopolymer of less reactive BPEA because of moderate conversion of the monomers (57–65%) insufficient for full consumption of more reactive AMPS.

Unfortunately, degree of branching cannot be evaluated from the analysis of ^{1}H NMR spectra. The peaks corresponding to the branching point in ^{1}H NMR spectra of BPAMPS in D_2O cannot be detected because of overlapping of the signal attributed to the methyl group in branching moiety (about 1.2 ppm [33]) with the strong and broad signal of two methyl groups in NaAMPS units (about 1.4 ppm). Obviously, the content of branching units in the branched NaPAMPS is less than the content of BPEA units since part of BPEA units are terminal. Nevertheless, the content of BPEA units is a good indicator of branching density in the branched NaPAMPS, i.e. branching density of NaPAMPS-24 is much higher than that of NaPAMPS-6.

Branched NaAMPS are transparent brittle solids soluble in water and methanol but insoluble in DMSO, pyridine and even pyridine – water mixture (1:1). They are colored, and the color changes from pale brown to saturated brown with increasing content of BPEA units.

3.2. Determination of molecular weight and conformation

SEC eluograms of the synthesized polyelectrolytes are shown in Fig. 3. Generally, unimodal but broad distributions of the SEC traces

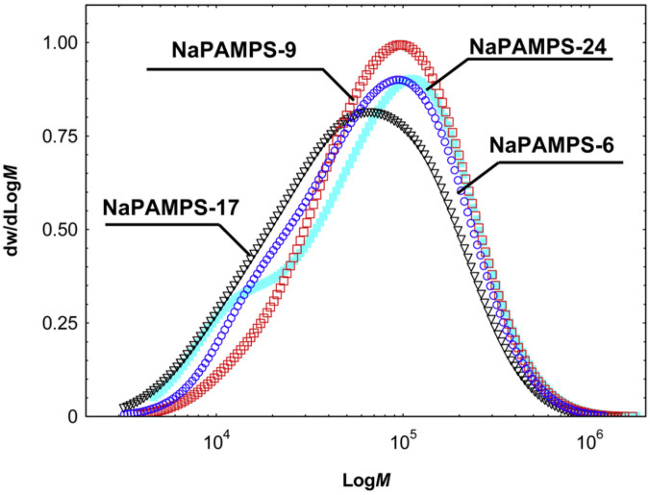

Fig. 3. SEC traces of the synthesized branched NaPAMPS.

were observed except for the polymer synthesized using the highest content of the *inimer* (NaPAMPS-24). Here, a small shoulder in the high-molecular weight region was found which might be attributed to a poorer solubility of *inimer*-rich macromolecules in the mixed water/pyridine solution.

Table 2 summarizes molecular parameters of the polyelectrolytes obtained by SEC measurements. AGET ATRP of NaPAMPS in the presence of the *inimer* BPEA resulted in high-molecular weight polymers with the values of the weight-average molecular weight 90000–120000 g/mol. Polydispersity of the synthesized branched polymers is rather high with the values close to $M_w/M_n \sim 2$ but this is typical for polymerization processes involving *inimers*. The polydispersity of NaPAMPS-24 reached the highest value $M_w/M_n = 2.47$ due to the highest amount of the *inimer* (30%) in the reaction mixture and slightly heterogenous conditions under polymerization.

The dependence of the radius of gyration R_g on weight-average molecular weight M_w for the sample NaPAMPS-9 is presented in Fig. 4. The slope values close to $a = 0.38–0.42$ are characteristic for highly branched/compact conformation. These data are in accordance with *arborescent* RAFT-polymers reported by Puskas et al. [18] whose conformational analysis yielded a slope of ~1/3.

Table 2
Molecular parameters of the branched NaPAMPS prepared by self-condensing AGET ATRP.

Sample	M_w	M_w/M_n	[a]R_g, nm	[b]a
NaPAMPS-6	112 000	1.99	26.0	0.42 ± 0.02
NaPAMPS-9	121 000	1.84	22.5	0.38 ± 0.02
NaPAMPS-17	95 000	1.98	27.4	0.42 ± 0.02
NaPAMPS-24	119 000	2.47	22.4	0.40 ± 0.03

[a] R_g - radius of gyration, estimation error ± 5 nm.
[b] a – conformation plot, slope.

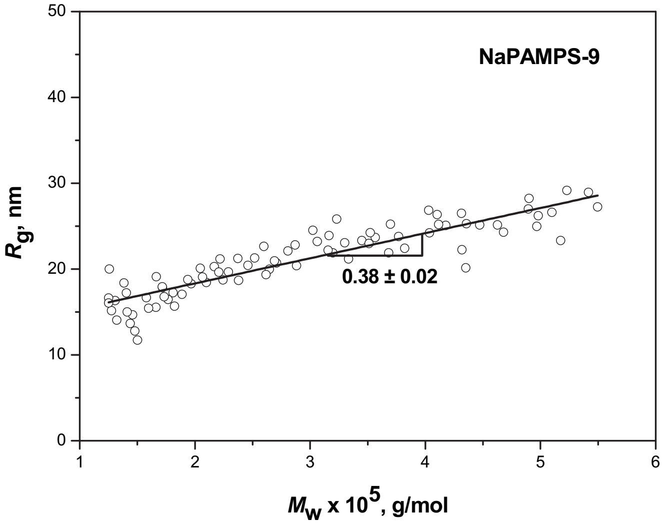

Fig. 4. Dependence of the radius of gyration R_g on weight-average molecular weight M_w for the sample NaPAMPS-9.

3.3. Dilute solution properties of *arborescent* NaPAMPS

Structure and dynamics of linear polylectrolytes with/without added low-molecular electrolytes were studied in a fairly large scope both theoretically [36–38] and experimentally [39–46]. In contrast, publications describing dilute solution properties of branched polyelectrolytes in general and *arborescent* in particular are scarce [47,48]. In the present study, a range of scattering techniques including small-angle X-ray scattering, dynamic and static light scattering were used to characterize *arborescent* NaPAMPS in aqueous solutions below cross-over concentration c^* defined by the classical formula:

$$c^*_{R_g} = M_w/(4\pi/3)N_A R_g^3 \tag{5}$$

where M_w is the weight-average molecular weight, N_A is the Avogadro number and R_g is the radius of gyration. The cross-over concentration c^* can be considerably different for polyelectrolytes without added salt and neutral polymers because of different chain conformation in the vicinity of c^* [22]. In other words, the transition from a state where polyelectrolyte chains are widely separated yet fully stretched to the state where they start to form entanglements leading to transient network can occur at much lower concentration.

Fig. 5 shows small-angle X-ray scattering (SAXS) profile of *arborescent* NaPAMPS-9 sample in 0.5 wt% solution ($c < c^*$) at relatively high ionic strength $C_S = 0.15$ M NaCl. The scattering data are represented as a Kratky plot corresponding to product of $I(q)q^2$ as a function of q. Addition of a salt ensures screening of electrostatic interactions leading to assumption that the scattering arises

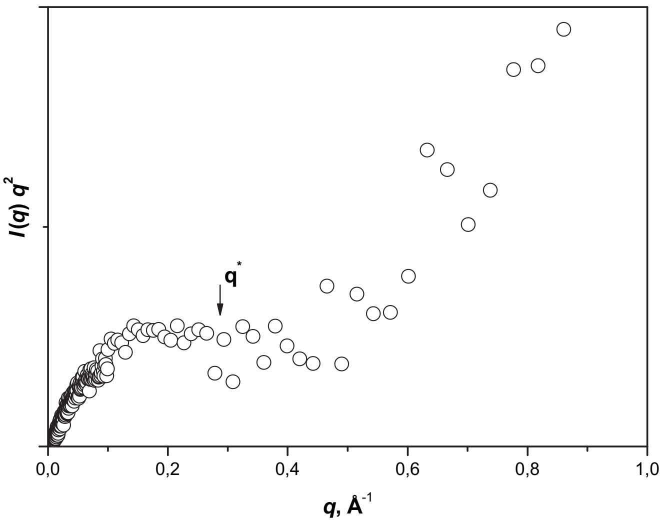

Fig. 5. Kratky plot of NaPAMPS-9 at $c = 0.5$ wt%.

from isolated, noninteracting chains where contributions of intramolecular effects are diminished. It is therefore clear that the bump at small q-range shall be interpreted as additional proof of branched and compact conformation and is not related to "polyelectrolyte peak" that would otherwise arise if the electrostatic repulsions would not be sufficiently screened. This reasoning allows calculation of the intrinsic persistence length, l_p by graphical analysis [49] using the value of $q^* = 0.28$ Å

$$l_p = 1.9/q^* \tag{6}$$

The calculated persistence length $l_p = 6.78$ Å corresponds roughly to the length of a monomer unit indicating flexible coillike behavior of NaPAMPS-9 chains.

The basic molecular parameters of the branched polyelectrolyte NaPAMPS-9 in dilute concentration regime has been determined by static light scattering using Zimm procedure. Typical Zimm plot is shown in Fig. 6, and the molecular parameters of the branched polyelectrolyte in 0.15 M NaCl aqueous solution are as follows: $M_w = 96300$, $R_g = 22.3$ nm and $A_2 = 9.35 \cdot 10^{-7}$ mol$\cdot$dm$^3\cdot$g^{-2}.

Both the weight-average molecular weight M_w and radius of gyration R_g are comparable with values obtained from SEC analysis given above (Table 2). A rather low value of the second virial coefficient $A_2 = 9.35 \times 10-7$ mol dm^3/g^2 indicates strong diminishing of excluded volume effect for this polymer at $C_S = 0.15$ M NaCl. In order to fully elucidate the effect of the salt concentration on the behavior of NaPAMPS-9 in dilute aqueous solution, a series of solutions were prepared with the salt concentrations spanning the range 0.005–0.1 (low ionic strength) and 0.1–2.0 (high ionic strength). The partial Zimm formalism was applied to extract the apparent radius of gyration $R_{g,app}$ which is plotted against salt concentration in Fig. 7.

At low ionic strength extensive coil expansion was demonstrated by high values of $R_{g,app}$ ~35.5–63.6 nm which however were not diminishing monotonically over the entire low ionic strength range upon addition of salt. A transition from "polyelectrolyte" behavior to "neutral" behavior occurs at $C_S = 0.15$ M NaCl. Further addition of the salt does not show substantial effect on $R_{g,app}$ values being in the range from 18 to 22 nm. Diffusive behavior of the studied solutions at high ionic strength was ascertained by DLS where the relaxation rate vs. q^2 obeyed a linear dependence (Fig. 8).

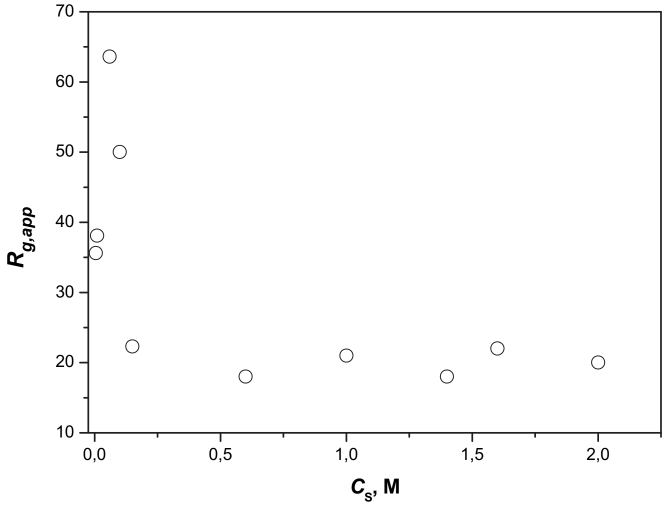

Fig. 7. Dependence of $R_{g,app}$ on salt concentration C_S (NaCl) for NaPAMPS-9.

This allows the translational difussion coeficient D to be determined using $\Gamma = Dq^2$. The dependence of the translational diffusion coefficient as a function of NaCl concentration is displayed in Fig. 9.

As can be seen from this graph at high ionic strength further addition of the salt has virtually no effect on D up to $C_S = 2$ M NaCl. The hydrodynamic radii R_h calculated by Stokes–Einstein relation are within $R_h = 11$–12 nm. The combination of $R_{g,app}$ and R_h yields dimensionless parameter defined as

$$\rho = R_{g,app}/R_h \tag{7}$$

which may serve as indicator of macromolecular conformation within investigated high ionic strength regime. The calculated values ρ fall between 1.63 and 2.08 which corresponds to a values characteristic for linear coil and are at the limit of rod-like behavior. This might be surprising since according to the synthesis procedure, conformational slope (a ~0.4) and Kratky plots quoted above, one shall expect more or less spherical architecture of the coil (predictions for the hard sphere behavior is $\rho = 0.776$) [6]. In addition, the electrostatic interactions are fully screened at high ionic strength, i.e. the charge effect is practically absent. Indeed,

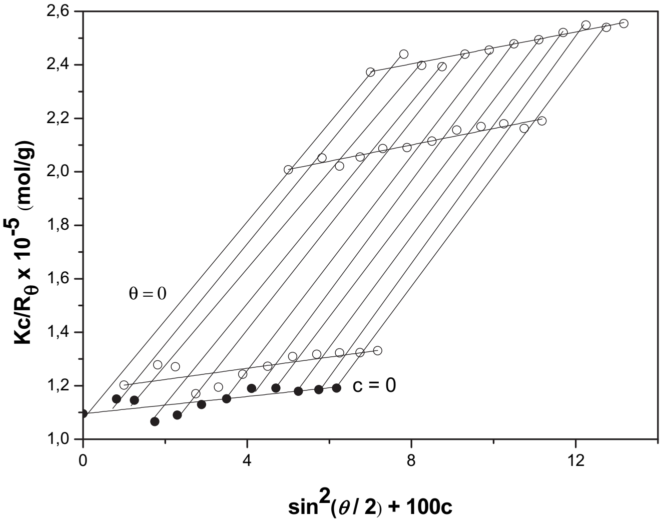

Fig. 6. Zimm plot for NaPAMPS-9 in aqueous solution at C_S = 0.15 M NaCl.

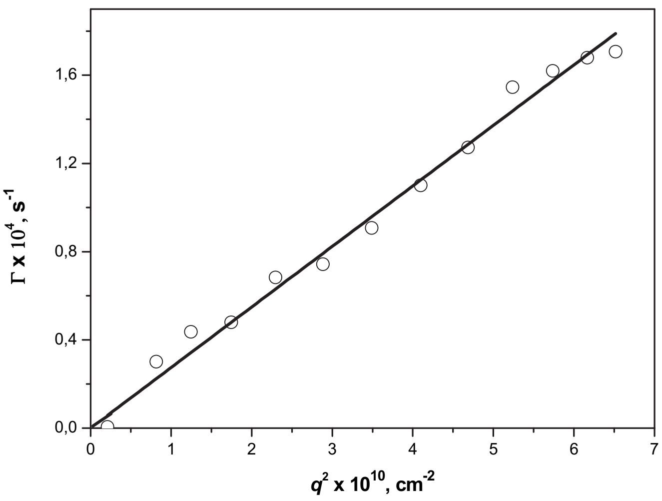

Fig. 8. Correlation function decay rate Γ as a function of squared scattering vector q^2 for the arborescent NaPAMPS-9 in water at C_S = 0.15 M NaCl.

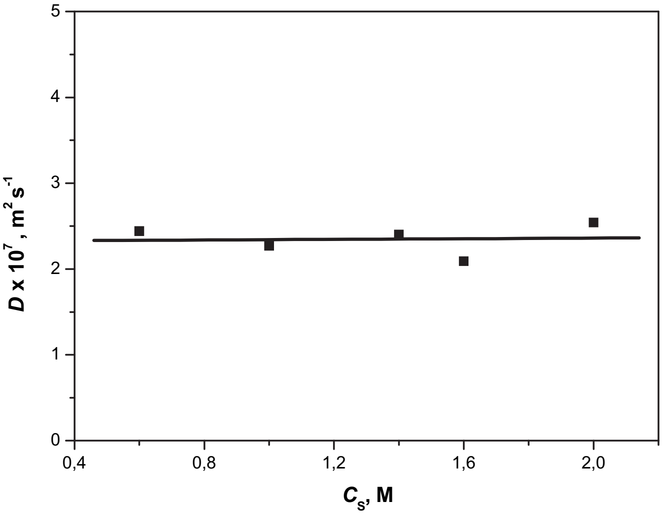

Fig. 9. Dependence of translational diffusion coefficient as a function of the salt concentration C_S for NaPAMPS-9.

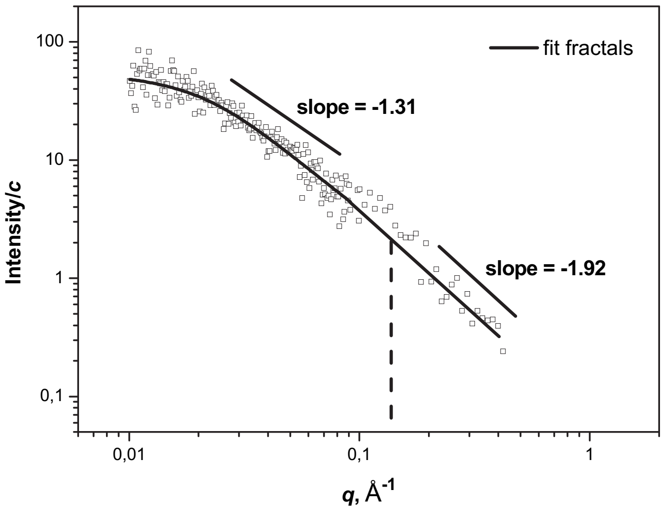

Fig. 11. SAXS curve for *arborescent* NaPAMPS-9 in water at $c = 0.5$ wt% with added salt ($C_S = 0.15$ M NaCl).

this can be concluded from Fig. 10 representing the dependence of D on concentration of NaPAMPS-9 in dilute concentration regime at $C_S = 0.15$ M NaCl. The translation diffusion coefficient increases with concentration in a manner which is characteristic for non-ionic polymers in a good solvent [6].

Thus, ρ parameter has to be analyzed with a great caution because, firstly, this value is a subject to experimental error in determination of R_g and, secondly, the polydispersity effect plays an important role [6]. In fact, R_g/R_h as a structure factor from batch experiments on polydisperse polymers may easily reach values 2 and higher because of comparison of different molecular weight averages. In other words, the effect of polydispersity on this ratio is much stronger than the effect of structure itself as clearly shown by Burchard [50].

Finally, the dilute solutions of NaPAMPS-9 at $C_S = 0.15$ M NaCl were analyzed by SAXS technique. Let us first look at intermediate region of the scattering curve (log–log plot) in Fig. 11.

The power law of the scattering intensity $I(q)$ can be described as $\sim q^{-1.31}$. This fractal dimension value lay in the region between thin cylinder and loosely branched conformations (or “fully swollen” chains). Then, in the high q-range domain ($q > 0.1$ Å^{-1}) we observe a slope transition from $q^{-1.31}$ to $q^{-1.92}$ indicated by a vertical dashed line on the graph. The behavior changes to a more dense structure corresponding to local blobs. Two scattering functions have been considered for fitting the SAXS curve, namely worm-like chain and dimensional analysis. The latter function was selected considering large contribution (70%) to the signal. The parameters characterizing the fit of the data are as follow: radius of gyration from Guinier plot $R_g = 67$ Å, contour length $L = 482$ Å, Kuhn length $b = 22$ Å, cross-section radius of gyration $R_{g,c} = 6$ Å, fractal dimension $f = 1.43$. According to theory, fractals with dimensions $f = 1.66$ correspond to a dense *arborescent* structure while $f = 1$ is a value characterizing thin rod. The determined fractal dimension $f = 1.43$ lays in between those values therefore we propose intermediate model for the prepared polyelectrolytes, namely, cylinders of average length connected into an *arborescent* structure.

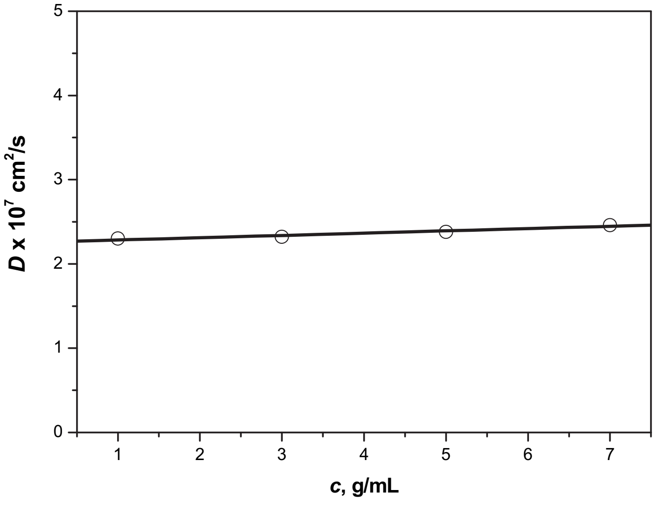

Fig. 10. Dependence of D on concentration of NaPAMPS-9 in dilute concentration regime at $C_S = 0.15$ M NaCl.

4. Conclusion

Self-condensing vinyl polymerization approach based on AGET ATRP mechanism have been succesfully used to synthesize *arborescent* poly(sodium 2-acrylamido-2-methyl-*N*-propanesulfonates) (NaPAMPS) in aqueous media for the first time. The content of branching units in the polyelectrolytes determined by ^{1}H NMR spectroscopy ranged from 6 to 24 mol %. The branched and compact structure of the synthesized *arborescent* polyelectrolytes was directly determined by SAXS experiments. The value of fractal dimension $f = 1.43$ obtained by fitting SAXS data was found to be in the intermediate range between rigid-rod and *arborescent* structure. The dependence of radius of gyration on weight-average molecular weight yielded the exponent $a = 0.38–0.42$ supporting branched structure of NaPAMPS polyelectrolytes and highlighting efficiency of the applied synthetic approach. It was found that the polyelectrolyte effect in dilute solutions can be effectively screened at salt concentration $C_S = 0.15$ M NaCl. It has to be said that *arborescent* polyelectrolytes prepared in this work are suitable model compounds for further experimental studies, for example, to validate predictions in scaling theory of semidilute and concentrated solutions of branched polyelectrolytes.

Acknowledgements

The authors wish to acknowledge the financial support offered by the European Commission through a Marie Curie Research

Training Network SOCON, MCRTN-CT-2004-512331. Financial support from the Research Council of Lithuania (Contract MIP-50/2010) is gratefully acknowledged. We thank Dr. A. Jigounov, Dr. P. Štěpánek and Dr. B. Porsch of Institute of Macromolecular Chemistry in Prague for numerous discussions and support of this work.

Appendix. Supplementary data

Supplementary data associated with this article can be found in the online version, at doi:10.1016/j.polymer.2010.09.058.

References

[1] Berwald S, Meier-Haack J. Handbook of polyelectrolytes and their applications. In: Tripathy SK, Kumar J, Nalwa HS, editors. Applications of polyelectrolytes and theoretical models, vol 3. American Scientific Publishers; 2002. p. 99.
[2] Matyjaszewski K, Gnanou Y, Leibler L. Macromolecular engineering: from precise macromolecular synthesis to macroscopic materials properties and applications. Weinheim: Wiley-VCH; 2007.
[3] Hawker CJ, Bosman AW, Harth E. Chem Rev 2001;101:3661.
[4] Matyjaszewski K, Xia J. Chem Rev 2001;101:2921.
[5] Moad G, Rizzardo E, Thang SH. Polymer 2008;49:1079.
[6] Gromadzki D, Lokaj J, Šlouf M, Štěpánek P. Polymer 2009;50:2451.
[7] Gromadzki D, Jigounov A, Štěpánek P, Makuška R. Eur Polym J 2010;46:804.
[8] Krivorotova T, Vareikis A, Gromadzki D, Netopilík M, Makuška R. Eur Polym J 2010;46:546.
[9] Fréchet JMJ, Henmi M, Gitsov I, Aoshima S, Leduc MR, Grubbs RB. Science 1995;269(5227):1080.
[10] Paulo C, Puskas JE. Macromolecules 2001;34:734.
[11] Baskaran D. Polymer 2003;44(8):2213.
[12] Simon PFW, Radke W, Müller AHE. Macromol Rapid Commun 1997;18:865.
[13] Hawker CJ, Fréchet JMJ, Grubbs RB, Dao J. J Am Chem Soc 1995;117:10763.
[14] Gaynor SG, Edelman S, Matyjaszewski K. Macromolecules 1996;29:1079.
[15] Matyjaszewski K, Gaynor SG, Müller AHE. Macromolecules 1997;30:7034.
[16] Mori H, Seng DC, Lechner H, Zhang M, Müller AHE. Macromolecules 2002;35:9270.
[17] Mori H, Walther A, André X, Lanzendörfer MG, Müller AHE. Macromolecules 2004;37:2054.
[18] Heidenreich AJ, Puskas JE. J Polym Sci Part A Polym Chem 2008;46:7621.
[19] Konkolewicz D, Gray-Weale A, Perrier S. J Am Chem Soc 2009;131:18075.
[20] Jakubowski W, Matyjaszewski K. Macromolecules 2005;38:4139.
[21] Gromadzki D, Filippov S, Netopilík M, Makuška R, Jigounov A, Pleštil J, et al. Eur Polym J 2009;45:1748.
[22] Sedlák M. Polyelectrolytes in solution. In: Brown W, editor. Static light scattering. Principles and Development. Clarendon: Oxford University Press; 1996. p. 120–65.
[23] Janata M, Kůdela V, Gromadzki D, Štěpánek P, Nallet F, Diat O, et al. e-Polymers 2006;055.
[24] Gromadzki D, Lokaj J, Černoch P, Diat O, Nallet F, Štěpánek P. Eur Polym J 2008;44:189.
[25] Gromadzki D, Makuška R, Netopilík M, Holler P, Lokaj J, Janata M, et al. Eur Polym J 2008;44:59.
[26] Masci G, Giacomelli L, Crescenzi V. J Polym Sci Part A Polym Chem 2005; 43:4446.
[27] Panova D, Mespouille L, Manolova N, Degée P, Rashkov I, Dubois P. Macromol Rapid Commun 2006;27:1489.
[28] McCullough L, Dufour B, Matyjaszewski K. J Polym Sci Part A Polym Chem 2009;47:5386.
[29] Sumerlin BS, Donovan MS, Mitsukami Y, Lowe AB, McCormick CL. Macromolecules 2001;34:6561.
[30] Förster S, Schmidt M. Adv Polym Sci 1995;120:51.
[31] Fisher LW, Sochor AR, Tan JS. Macromolecules 1977;10:949.
[32] Fisher LW, Sochor AR, Tan JS. Macromolecules 1977;10:955.
[33] Matyjaszewski K, Gaynor SG, Kulfan A, Podwika M. Macromolecules 1997;30:5192.
[34] Wittgren B, Porsch B. Carb Polym 2002;49:457.
[35] Kazantsev OA, Igolkin AV, Shirshin KV, Kuznetsova NA, Spirina AN, Malyshev AP. Russ J Appl Chem 2002;75:465.
[36] de Gennes PG, Pincus P, Velasco RM, Brochard F. J Physique 1976;37:1461.
[37] Odijk T. Macromolecules 1979;12:688.
[38] Odijk T. J Polym Sci Polym Phys Ed 1977;15:477.
[39] Grüner F, Lehmann WP, Fahlbusch H, Weber R. J Phys A Math Gen 1981;14:L307.
[40] Sedlák M, Koňak Č, Štepanek P, Jakeš J. Polymer 1987;28:873.
[41] Förster S, Schmidt M, Antonietti M. Polymer 1990;31:781.
[42] Sedlák M, Amis EJ. J Chem Phys 1992;96:817.
[43] Sedlák M, Amis EJ. J Chem Phys 1992;96:826.
[44] Tanahatoe JJ, Kuil ME. J Phys Chem B 1997;101:9233.
[45] Buhler E, Boué F. Eur Phys J E 2003;10:89.
[46] Cong R, Temyanko E, Russo PS, Edwin N, Uppu RM. Macromolecules 2006;39:731.
[47] Gauthier M. J Polym Sci Part A Polym Chem 2007;45:3803.
[48] Yun SI, Gruber RM, Kee RA, Gauthier M. Polymer 2006;47:2750.
[49] Glatter O, Kratky O. Small angle X-Ray scattering. London: Academic Press; 1982.
[50] Burchard W. Adv Polym Sci 1999;143:113.